Synthesis and structural characterization of $NiS_{2-x}Se_x$ thin films

1998 J. Phys.: Condens. Matter 10 6919

(http://iopscience.iop.org/0953-8984/10/31/010)

J. Phys.: Condens. Matter **10** (1998) 6919–6930. Printed in the UK PII: S0953-8984(98)91540-5

Synthesis and structural characterization of $NiS_{2-x}Se_x$ thin films

R Otero†, J L Martín de Vidales‡ and C de las Heras†

† Dpto Física de Materiales (C-IV) and Instituto Nicolás Cabrera, Universidad Autónoma de Madrid, 28049-Madrid, Spain

‡ Dpto C-VI Facultad de Ciencias, Universidad Autónoma de Madrid, 28049-Madrid, Spain

Received 11 February 1998

Abstract. $NiS_{2-x}Se_x$ thin films in the range $0 \leqslant x \leqslant 2$ have been synthesized by sulphuration/seleniation of Ni thin films thermally evaporated on glass substrates. Growth conditions of temperature, time and pressures have been established to obtain samples with different selenium content and a theoretical model of the process has been proposed. Structural properties of the films are studied by Rietveld refinement of x-ray diffraction data. Values of lattice constant, a, sulphur/selenium positional parameter, u, and Se content in $NiS_{2-x}Se_x$ solid solution have been obtained. Moreover, Ni–anion and anion–anion bond distances have been obtained and analysed in relation to the selenium in the samples. It has been found that the lattice parameter follows a Vegard law with the selenium content. Resistivity measurements as a function of temperature from 10 to 200 K have been obtained for samples with $x = 0.22$ and $x = 0.40$ respectively. A change in the resistivity behaviour is evident in the sample with $x = 0.40$ at $T \sim 100$ K, which can be associated with a phase transition observed in single crystals with the same Se content.

1. Introduction

Transition metal dichalcogenides with pyrite-type structure have recently received considerable attention because they present interesting electric and magnetic properties. In particular the $NiS_{2-x}Se_x$ system has interesting transport properties due to the different electrical character for the two end members of the series: semiconductor (NiS_2) and metallic ($NiSe_2$) behaviour respectively. Some works have been published in relation to properties of $NiS_{2-x}Se_x$ single crystals [1–11] in recent years, reporting that depending on the selenium content it is possible to find samples with semiconductor properties ($x < 0.26$) or metallic ones ($x > 0.6$) [1], showing in the range $0.4 \leqslant x \leqslant 0.58$ a Mott–Hubbard metal–insulator transition [2, 3]. By application of an external pressure the system also changes its conduction behaviour from semiconductor to metallic, and the relation has been observed between the transition pressure and the selenium content in the sample [5]. This shows the importance that structural and mechanical features have on all other properties and the interest in comparing the properties of the thin film with those reported before for single crystals in bulk.

By Hall effect measurements on NiS_2, T Thio and J W Bennett [4] concluded that at low temperatures, transport properties are dominated by metallic surface layers. In this sense the study of properties of this material in a thin film would reveal interesting conclusions about its behaviour.

0953-8984/98/316919+12$19.50

To date, we have no knowledge on synthesis and characterization of materials included in the $NiS_{2-x}Se_x$ solid solution prepared as thin films. In addition, thin film synthesis of sulphides by sulphuration of the metal film is a technique that has been used successfully in other pyrites synthesis [12].

The aim of this work is to establish the $NiS_{2-x}Se_x$ thin film growth conditions to obtain samples with different x values in the range $0 \leqslant x \leqslant 2$ and principally for those values near to $x = 0.5$. Selenium content, structural and electrical properties of the samples are analysed by using different techniques. Obtained data for the films are compared to those reported for single crystals with the same selenium content.

2. Experiment

2.1. Sample preparation

$NiS_{2-x}Se_x$ thin films were prepared by sulphuration and seleniation at the same time of nickel thin films thermally evaporated on a glass substrate. The method is analogous to that used in FeS_2 thin film preparation [12]. Nickel films were deposited using an Edward Auto 306 coating system by thermal evaporation of Ni powder of 100 μm size on glass substrates that had been previously degassed at 520 K in a vacuum of 10^{-6} Torr. During the nickel evaporation the glasses were maintained at 470 K and the film thickness was monitoring by a FTM 5 monitor with a quartz microbalance. After the evaporation, the film thickness was measured by a Dektak profilometer and the values obtained were about 0.20 ± 0.02 μm.

Nickel films were submitted to a sulphuration and seleniation by heating the samples in sealed ampoules in a sulphur–selenium mixing atmosphere. The heating temperature was in the range 620 to 720 K and was maintained for 10 or 20 hours respectively. The theoretical total pressure (sulphur + selenium, P_t) was variable from 300 to 4000 Torr. The selenium partial pressure was from 25 to 100% of the total pressure (P_t). Although spectrometry studies of both gases reveal that the equilibrium composition of the vapour contains molecules with a higher number of atoms at those temperatures [13, 14], sulphur and selenium amounts introduced into the ampoule to maintain the different partial pressures were calculated by considering as diatomic the sulphur and selenium molecules in the gas. According to those pressures, amounts introduced into the ampoule have been calculated by considering the perfect gas equation. The selenium partial pressure has been calculated by applying the Dalton law. Sample thickness increases during the treatment up to values in the range of 0.4 to 0.7 μm for the different obtained samples.

The selenium contained in the samples was measured with a total reflection x-ray fluorescence (TXRF) Extra II, Seifer, with two x-ray lines, Mo and W anodes and Si detector.

2.2. X-ray powder diffraction analysis and structure refinement

X-ray diffraction diagrams of the films were recorded in a Siemens D5000 diffractometer in the usual θ–2θ couple mode with monocromatized Cu Kα ($\lambda = 1.5418$ Å) radiation, working at 40 kV and 30 mA. A secondary graphite monochromator served to suppress the Cu Kβ radiation. All diagrams were collected from 20° (2θ) to 120° (2θ) in the step scanning mode, with a 0.02° (2θ) step scanning and 2 s counting time. Divergence slits located in the incident beam were selected to ensure complete illumination of the specimen surface at 15° (2θ). All x-ray experiments were carried out at 293 ± 1 K.

X-ray powder diffraction patterns showed that all synthesized materials are of $NiS_{2-x}Se_x$ solid solution crystallized with pyrite type structure in the space group $Pa3$ (No 205) with $Z = 4$. The two binary end members of solid solution NiS_2 and $NiSe_2$ present cell dimensions 5.670 Å (JCPDS, file 11-99) and 5.991 Å (JCPDS, file 11-1495), respectively.

The least-square structure refinements were undertaken with the full-profile, Rietveld type, program DBWS-9006PC, prepared by Sakthiveld and Young [15]. A Pearson-VII function was used for the representation of the profiles. The refined quantities in all samples were C-scale factor, 2θ zero shift parameter, five background parameters, a peak full width at half maximum (FWHM) function described by the usual quadratic form [16]:

$$(\mathrm{FWHM})^2 = U\tan^2\theta + V\tan\theta + W \tag{1}$$

where U, V and W are the refinable parameters, the peak asymmetry parameter, the unit cell constant a, the fractional atomic coordinate u for the anion in the lattice and Se content (x) in the $NiS_{2-x}Se_x$; for this latter determination, $\Sigma(\mathrm{S} + \mathrm{Se})$ in the $NiS_{2-x}Se_x$ formula was constrained to 2.0. Finally, the isotropic thermal parameters B_{Ni} and B_{anion} were also refined. Strategies followed during the Rietveld refinements and the mean of several agreement R-factors are similar to those gathered in [12]. Selected bond distances have been determined from the structural parameters (a and u) taking into account the symmetry operations in the space group $Pa3$.

As an example of the refinement, in table 1 the final Rietveld refinement parameters for the $NiS_{2-x}Se_x$ sample prepared from nickel films by sulphuration/seleniation at 773 K for 20 h, with $P_t = 500$ Torr and 0.6 molar fraction of selenium, are presented. Selenium content in the sample has been determined as 0.4. Figure 1 shows a plot of the observed, calculated and difference profiles for the final Rietveld refinement of this sample.

Table 1. Final Rietveld refinement parameters for $NiS_{1.60}Se_{0.40}$ phase prepared at 773 K for 20 h (sample 14).

Profile function used	Pearson VII	
Space group	$Pa3$	
Cell parameter	$a = 5.7472(2)$ Å	
Positional parameter	$u = 0.3920(4)$	
Number of Se atoms	$N(\mathrm{Se}) = 0.40(3)$	
Isotropic temperature factors	$B(\mathrm{Ni}) = 1.1(1)$ Å^2	
	$B(\mathrm{S}) = B(\mathrm{Se}) = 0.74(9)$ Å^2	
Pearson VII parameter	$m = 2.2(1)$	
Asymmetry parameter	$\eta = 1.7(3)$	
FWHM function parameter	$U = 0.195(5)$	
	$W = 0.0158(9)$	
Zero shift (2θ)	0.101(1)	
Scale factor	0.23×10^{-5}	
Background parameters	$B_0 = 247(3)$, $B_1 = -11.6(2)$, $B_2 = 0.215(4)$	
	$B_3 = -0.0017(3)$, $B_4 = (0.53(1)) \times 10^{-7}$	
Agreement indices	R_p	17.06
	R_{wp}	23.62
	$R_{expected}$	20.58
	R_{Bragg}	10.60
	$R_{structure\ factor}$	11.20
	Goodness of fit (GF)	1.15

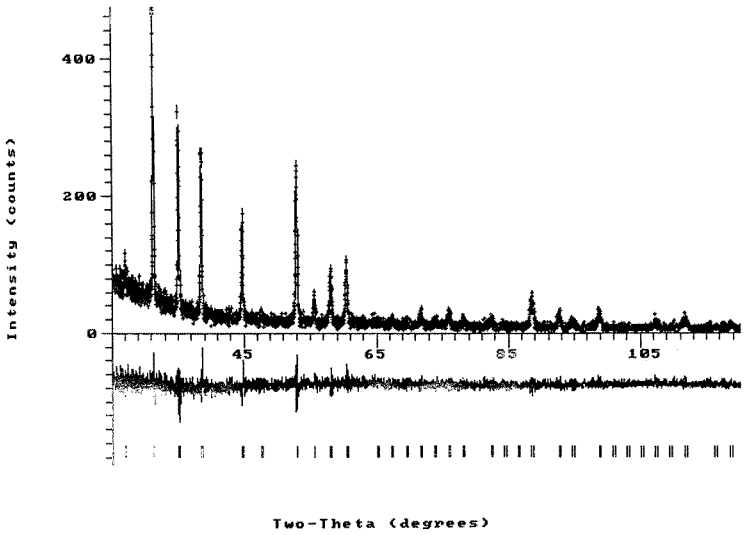

Figure 1. The final Rietveld refinement plot of $NiS_{1.6}Se_{0.4}$ (no 14 in table 3) thin film prepared at sulphuration/seleniation of 773 K for 20 h with $P_t = 500$ Torr and a molar fraction in gas 0.6. The upper trace shows the observed x-ray diffraction intensity data as crosses, and the calculated pattern is shown by solid line. The lower trace is a plot of the difference observed minus calculated. The vertical markers show positions calculated for Bragg reflections.

2.3. Resistivity measurements

Resistivity measurements were made at temperatures varying from 10 to 300 K by the four probe method. The sample was introduced into a liquid-helium variable-temperature cryostat similar to that described by Gmelin and v Alpen [17], which guarantees a great temperature stability.

3. Results

3.1. Structure

3.1.1. NiS_2 samples. A series of NiS_2 films has been synthesized by sulphuration of Ni films at temperatures in the range of 630–770 K and at pressures of 300 and 5000 Torr. A structural analysis of the obtained samples has been made by Rietveld refinement of x-ray diffraction intensities and the results are presented in table 2. Values of lattice parameters, sulphur positional parameters and S/Ni relations are presented in addition to growth conditions of temperature and pressure. Also, values of Ni–S and S–S bond distances are included. Samples sulphurated at a pressure of 300 Torr and temperatures in the range of 630 to 770 K show variations of 0.08% in the lattice parameter, a, and 0.80% in the sulphur positional parameter, u. On the other hand, values for the S/Ni relation are in the range 1.91 to 2.08. It is important to point out that variations of the a and u parameters found in this work are much lower than those observed in samples of FeS_2 [12] obtained by the same preparation method and temperature range (0.1% in a, 1.6% in u). Variations in the S/Ni relation is about 8%, similar to the variation in S/Fe relation for FeS_2 samples in the same range (10% in S/Fe). However, for the sample number 5 where Ni vacancies

Table 2. Growth conditions, thickness and summary of the obtained results by Rietveld refinement of x-ray diffraction of NiS_{2-x} samples. Values of Ni/S relation, lattice parameter a, sulphur positional parameter u and atomic bond distances Ni–S and S–S respectively are presented.

Sample	T (K)/t (h)	P_t (Torr)	d (μm)	S/Ni	a (Å)	u	Ni–S (Å)	S–S (Å)
1	623/10	300	0.46(1)	1.97(4)	5.6861(4)	0.3934(6)	2.396(4)	2.100(5)
2	673/10	300	0.32(1)	2.02(3)	5.6860(2)	0.3937(5)	2.398(3)	2.080(4)
3	723/10	300	0.45(1)	1.96(3)	5.6863(1)	0.3935(5)	2.397(3)	2.092(4)
4	773/10	300	0.45(1)	1.93(2)	5.6881(1)	0.3934(4)	2.399(3)	2.083(4)
5	723/10	300	0.46(1)	2.07(3)	5.6835(2)	0.3966(7)	2.402(3)	2.036(4)
6	723/10	5500	0.47(1)	1.91(2)	5.6871(1)	0.3940(5)	2.397(3)	2.088(4)

seem to be observed (S/Ni = 2.08), a more important lattice diminution ($a = 5.6835$ Å) is shown in relation to other samples. These results are in agreement with previous ones [7].

3.1.2. $NiS_{2-x}Se_x$ samples. $NiS_{2-x}Se_x$ samples have been synthesized by heating Ni films at temperatures in the range 723–773 K for 10 and 20 h respectively in a sulphur and selenium mixing atmosphere.

Hereafter, we will use the notation x_g to indicate twice the molar fraction of selenium in the vapour phase and x_{Se} for selenium content in the samples. The reason is that x_{Se} is the number of selenium atoms for each Ni atom, i.e, the number of selenium atoms for each two atoms of the total (S + Se). But in the gas phase, the number of selenium atoms for each two of the total (S + Se) is twice the molar fraction of selenium.

Table 3 shows results of some structural parameters obtained from Rietveld refinement of x-ray powder diffraction patterns in synthesized $NiS_{2-x}Se_x$ ($0 \leqslant x \leqslant 2$) thin films. Growth parameters, total pressure P_t, twice selenium molar fraction x_g and temperature and time of the sulphuration/seleniation are also included. For all structural parameters, standard deviations of the parameter values obtained from refinements are indicated in parentheses. Moreover, thickness and crystallite size of all the samples are also shown.

As can be observed (table 3), the samples have been obtained at different total pressures (250–4500 Torr) and different selenium molar fraction (0.18–1.00). It has been observed that, maintaining a constant value of 0.25 for the selenium molar fraction in the gas ($x_g = 0.5$) (samples 1–6), an increase in the total pressure, P_t, increases the selenium content in the sample up to $x_{Se} = 0.2$ for $P_t = 500$ Torr. For higher P_t values, the selenium contents in the samples measured by fluorescence and determined by x-ray diffraction keep constant.

Figure 2 presents selenium content (x_{Se}) in samples as a function of twice the molar fraction x_g in the gas, which has been calculated to obtain the different partial pressures by maintaining constant the total pressure at 500 Torr at the sulphuration/seleniation temperature. Values of selenium content included in the plot have been obtained by x-ray fluorescence and determined by x-ray diffraction respectively. As can be observed values of x_{Se} relation obtained by both methods are very similar. Also it can be appreciated that the selenium content in the sample increases slowly with respect to the amount in the gas up to reach a value of 0.5 and afterward the increase up to $x_{Se} = 2.0$ is fast. Experimental values are fitted by a theoretical relation taking into account the different states in which the sulphur and selenium atoms can be found during the process: in gas, on the substrate surface and in the bulk respectively (see the discussion).

Table 3. $NiS_{2-x}Se_x$ samples. Summary of the growth conditions and obtained results by Rietveld refinement of x-ray diffraction: temperature T, time t, total pressure (S + Se) P_t, two times molar fraction of selenium in gas x_g, thickness d, selenium content in the sample determined by x-ray diffraction x_{Se}, lattice parameter a, anion positional parameter u and grain size.

Sample	T (K)/t (h)	P_t (Torr)	x_g	d (μm)	x_{Se} XRD	a (Å)	u	Grain size (Å)
1	723/10	4475	0.4	0.44(1)	0.12(2)	5.7051(2)	0.3923(5)	745
2	723/10	1550	0.5	0.36(1)	0.19(3)	5.7052(4)	0.3934(5)	525
3	773/10	750	0.5	0.71(1)	0.11(2)	5.7049(2)	0.3933(4)	700
4	773/10	500	0.5	0.42(1)	0.14(2)	5.7118(2)	0.3943(4)	675
5	723/10	300	0.5	0.65(1)	0.10(2)	5.7075(2)	0.3930(5)	575
6	723/10	250	0.5	0.35(1)	0.07(3)	5.6944(5)	0.3926(7)	500
7	773/10	250	0.8	0.50(1)	0.25(2)	5.7212(3)	0.3930(6)	860
8	723/10	250	0.5	0.50(1)	0.14(3)	5.7105(2)	0.3933(6)	1000
9	723/20	500	0.8	0.65(1)	0.21(3)	5.7190(2)	0.3931(6)	850
10	723/20	500	1.0	0.47(1)	0.32(3)	5.7285(2)	0.3922(4)	815
11	723/20	500	1.1	0.50(1)	0.38(2)	5.7478(2)	0.3914(7)	710
12	723/20	500	1.2	0.40(1)	0.36(2)	5.7318(4)	0.3938(4)	730
13	758/20	500	1.2	0.55(1)	0.27(2)	5.7351(2)	0.3919(5)	700
14	773/20	500	1.2	0.50(1)	0.40(3)	5.7472(2)	0.3920(4)	660
15	723/20	500	1.3	0.60(1)	0.33(3)	5.7374(2)	0.3920(4)	725
16	723/20	500	1.4	0.45(1)	0.45(3)	5.7533(2)	0.3828(4)	670
17	723/20	500	1.56	0.52(1)	1.01(4)	5.8031(2)	0.3925(3)	680
18	723/20	500	1.6	0.45(1)	1.34(6)	5.8688(3)	0.3667(3)	790
19	723/20	500	1.7	0.60(1)	1.74(6)	5.8969(2)	0.3853(3)	915
20	723/20	500	1.9	0.60(1)	1.93(5)	5.9382(2)	0.3855(3)	950
21	723/20	500	2.0	0.70(1)	2.00	5.959 91(6)	0.3838(3)	1400

Figure 3 shows the unit cell length as a function of selenium content x_{Se}. As can be seen, there is a linear relationship between a and x_{Se} with a correlation coefficient of 0.994. This result clearly indicates that a Vegard law is followed and it is described by the equation:

$$a = (5.6916 + 0.128\ x_{Se})\ \text{Å}. \tag{2}$$

The anion positional parameter u also follows a linear dependence with selenium content, given by

$$u = 0.394 - 0.0049\ x_{Se} \tag{3}$$

with $r = 0.95$.

Figure 4 shows Ni–A and A–A bond distances (A = S or Se anion) as a function of selenium content, x_{Se}. In both cases, these parameters show a high correlation with x_{Se}. Recently [12], it has been pointed out that the anions in pyrite type structure show distances between the nearest neighbours d(A–A) and d(Ni–A) that depend on two parameters: the unit cell dimension, a, and the anion positional parameters u, expressed as follows:

$$d(\text{A–A}) = 2a\sqrt{3}(0.5 - u) \tag{4}$$

$$d(\text{Ni–A}) = a(3u^2 - 2u + 0.5)^{1/2}. \tag{5}$$

Thus, the structural parameters a and u (table 3), can be used to determine bond length values. On the other hand, from (2) and (3) it is possible to express the unit cell length as a function of d(A–A) and d(Ni–A) as follows:

$$a = d(\text{A–A})/\sqrt{3} + [4d(\text{Ni–A})^2 - 2d(\text{A–A})^{2/3}]^{1/2}. \tag{6}$$

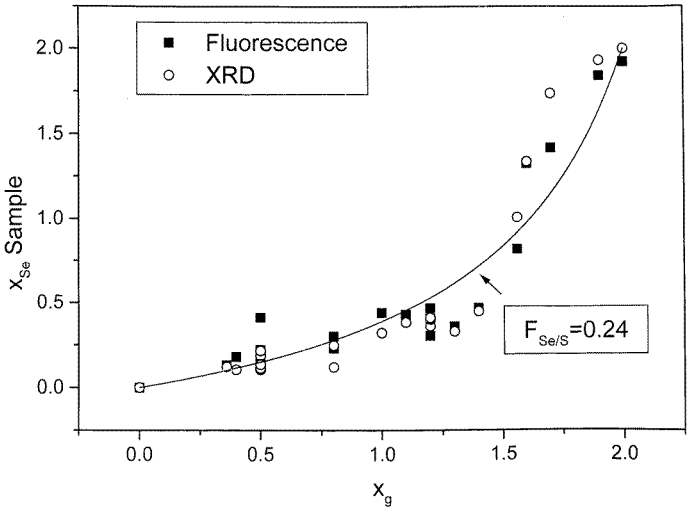

Figure 2. Selenium content in $NiS_{2-x}Se_x$ thin films measured by x-ray fluorescence (■) and determined by x-ray diffraction (○) as a function of two times the molar fraction of selenium in the gas (x_g). The solid line is the best fit of expression (9) to experimental data, with $F_{Se/S} = 0.24$, obtained by the least squares method.

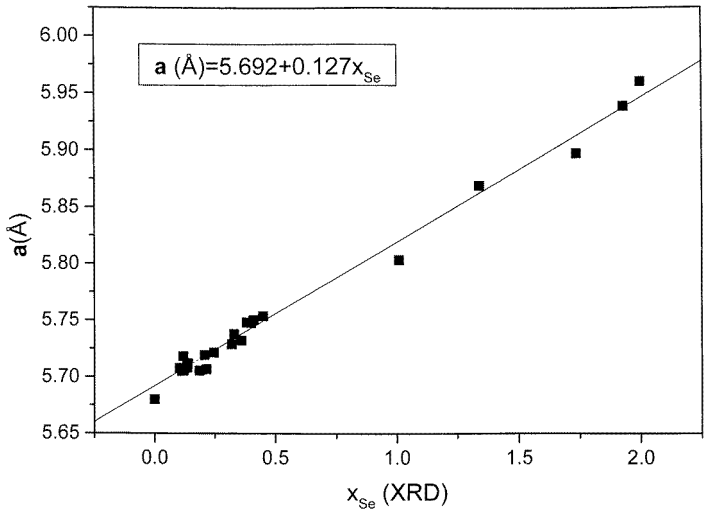

Figure 3. Lattice parameter a as a function of the selenium content in prepared thin films determined by x-ray diffraction. Notice a Vegard law is followed.

This last relation indicates that for stoichiometric NiS_2 and $NiSe_2$ pyrite type structures, bond distances, i.e., $r(S^-)$, $r(Se^-)$ and $r(Ni^{2+})$ effective radii, should be invariant and the unit cell length would remain constant. Thus, variations in a and u parameters may be related to Se by S isomorphic substitution in the $NiS_{2-x}Se_x$ solid solution. d(A–A) and d(Ni–A) vary respectively from 2.080(4) and 2.395(3) Å for the NiS_2 phase to 2.3990(25) and 2.488(2) Å for the $NiSe_2$ ones.

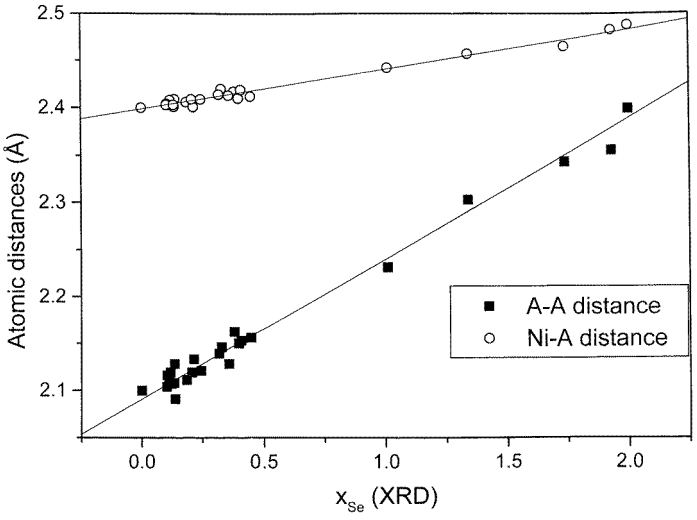

Figure 4. Atomic bond distances Ni–anion (○) and anion–anion (S or Se) (■) nearest neighbour as a function of selenium content in samples as determined by x-ray diffraction. The solid lines are linear fittings with expressions d(A–A) $= 2.091 + 0.149\ x_{Se}$ ($r = 0.980$) and d(Ni–A) $= 2.3989 + 0.042\ x_{Se}$ ($r = 0.990$) respectively.

Taking into account all data for synthesized thin films, we obtain two linear relations that can be written as follows:

$$d(\text{A–A}) = 2.091 + 0.149\ x_{Se} \tag{7}$$

and

$$d(\text{Ni–A}) = 2.3989 + 0.042\ x_{Se} \tag{8}$$

with r values 0.980 and 0.990 respectively.

3.2. Resistivity

Resistivity measurements have been carried out on two selected samples with $x_{Se} = 0.22$ and 0.40 respectively, as determined by x-ray diffraction. Samples with these selenium contents have been chosen because, in single crystals, samples with $x_{Se} = 0.22$ are semiconductors and the metallic–insulator transition has not been observed whereas for $x_{Se} = 0.40$ it has been. Resistivity measurements were carried out between 10 and 300 K with values varying from 10^{-2} to $4 \times 10^{-2}\ \Omega$ cm. Figure 5 shows a plot of resistivity against temperature for samples with $x_{Se} = 0.22$ and 0.40, respectively. As can be seen, while the sample with $x_{Se} = 0.22$ shows a semiconductor behaviour for any temperature (figure 5(a)), the sample with $x_{Se} = 0.40$ shows a metallic behaviour up to about 100 K; at this temperature a metallic–insulator transition occurs (figure 5(b)). In the metallic range, the shape of the plot agrees well with single crystal data [1, 3, 8]. This can be expected due to the large crystallite size of the samples (see table 3), and in metallic polycrystalline films the crystallite resistivity is dominant in relation to that of the boundary [18]. However, in the semiconducting regime differences are found because to the resistivity in polycrystalline semiconductor films is principally controlled by grain boundary barriers [19] and then it will increase in relation to the single crystal samples.

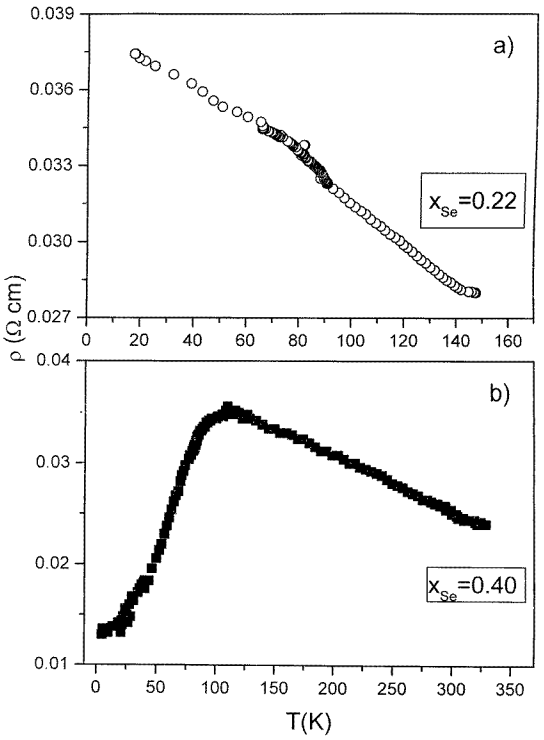

Figure 5. Electrical resistivity as a function of temperature for two samples with different selenium content (a) $x_{Se} = 0.22$ (○) and (b) $x_{Se} = 0.40$ (■). In (a) we observe a semiconducting behaviour between 10 and 200 K, but in (b) we find a Mott metal–insulator transition near 90 K.

4. Discussion

Thin films here obtained present a selenium content running over a wide range and show similar properties to those reported in single crystals. However from these results it can be concluded that there are differences in the sulphur and selenium diffusion into the sample. To understand the relation between the selenium amount introduced into the ampoule and that which is obtained in the sample see figure 2, we propose the following model. First, an adsorption process occurs and molecular selenium and sulphur arrive at the substrate and become trapped on the surface. Afterward the selenium and sulphur adsorbed can pass through the surface into the bulk. Then the scheme of the process can be represented as follows:

$$\begin{array}{ccccc} & \overset{A}{\Rightarrow} & & \overset{C}{\Rightarrow} & \\ \text{Gas} & & \text{Adsorbed} & & \text{Absorbed} \\ \text{state} & \overset{B}{\Leftarrow} & \text{state} & & \text{state} \end{array}$$

where A is the inverse of the mean time for a molecule in the gaseous state to be adsorbed by the surface. The number of molecules adsorbed by the surface per unit time and area, at a pressure P and temperature T, can be written as $P/(2\pi M k_B T)^{1/2}\alpha$ (α is the sticking coefficient, M the mass of the adsorbed molecule and k_B the Boltzmann constant) [20]. Then, A can be expressed as $A = (S/V)(k_B T/2\pi M)^{1/2}\, \mathrm{e}^{E(ads)/kT}$, where we have supposed

$\alpha = e^{E(ads)/kT}$, with E(ads) the height of the potential well of the adsorbed state, and S and V are the surface and volume of the sample respectively.

B is the inverse of the mean time for a molecule in the adsorbed state to escape from the surface into the gas. Supposing a parabolic well, the adsorbed molecule will be oscillating with a period $\tau = (K/M)^{1/2}$ (K is the Hooke constant associated with the potential well and M is the molecule mass). According to Boltzmann's law this molecule will have the required energy to escape (E(ads)) for a fraction of time equal to $e^{E(ads)/kT}$, so the mean time is $(K/M)^{1/2}\, e^{E(ads)/kT}$ and $B = (M/K)^{1/2}\, e^{-E(ads)/kT}$.

Finally, C is the inverse of the mean time for a molecule adsorbed in the surface to penetrate the bulk. Its value is $C = (M/K)^{1/2}\, e^{-E(abs)/kT}$.

The model is based on the following hypothesis:

(a) Se and S partial pressures were supposed constant during the process. This can be done, due to the great amount of gas molecules into the ampoule compared to those which can go into the nickel film.

(b) It is supposed that the height of the potential well of adsorption is smaller than the energy barrier to penetrate the bulk. So, the process of bulk absorption is slower than the process of surface adsorption, and, due to the great amount of molecules in the gas, the equilibrium number of adsorbed molecules in the surface is quickly re-established. Then the number of adsorbed molecules on the surface will be considered constant too. In addition to this, we neglect the possibility for absorbed molecules to leave the bulk because we consider the adsorption places nearly occupied and the energy barrier to leave the bulk greater than the one to be absorbed.

(c) Finally, we suppose a finite number of adsorption and absorption sites, respectively. The kinetic equations are solved for a process that is represented in the scheme by considering the velocities of each process as not only proportional to the molecule number in the first state, but also to the fraction of free places in the final state. The result of the selenium content on the bulk is:

$$x_{Se} = 2F_{Se/S}x_g/[(F_{Se/S} - 1)x_g + 2] \tag{9}$$

where $F_{Se/S} = F_{Se}/F_S$ and $F = CA/B$.

$F_{Se/S}$ is an adjustable parameter, which fits well to the experimental data with a value of 0.24, and it is related to the different facilities for selenium and sulphur to penetrate the fcc lattice of nickel. The theoretical curve is plotted in figure 2 and can be observed to fit well with the main features of the experimental data.

On the other hand, the lattice parameter follows very accurately a Vegard law with selenium content. Also the u parameter follows a linear relation with the selenium content. Taking into account relations (4) and (5), bond distances should present a non-linear dependence on selenium content. By substitution of expressions (2) and (3) obtained for a and u into (4) and (5) respectively, we obtain

$$d(\text{A–A}) = 2.090 + 0.144x_{Se} + 6.3 \times 10^{-4}\, x_{Se}^2 \tag{10}$$

and

$$d(\text{Ni–A}) \approx 2.401 + 4.2 \times 10^{-2}x_{Se} + 6.5 \times 10^{-4}\, x_{Se}^2. \tag{11}$$

It can be seen from (10) and (11) that the quadratic term in x_{Se} is rather small. This is the reason why a linear relation fits well the experimental results in figure 4 and the obtained coefficients in relations (7) and (8) for the other terms are very similar to those predicted by (10) and (11) respectively. Notice also in figure 4 that selenium presence is

more important for d(A–A) than for d(Ni–A). In fact, the slope of the linear fit (7) is three times greater than that of (8).

Due to the symmetric situation of both atoms of S/Se dimers, it is clear that their bond is mainly of covalent character. In spite of this, their bond distance is greater than twice the covalent radius (the covalent radius for S is 1.02 Å, and d(S–S) in NiS_2 is ≈2.1 Å (7)). This fact can be explained due to the distorted tetrahedral coordination site of each sulphur atom. If we suppose that all Ni atoms are point charges with two units of atomic charge and that the covalent bond between the S^- ions is a parabolic potential well, the presence of Ni^{2+} ions will produce an enlargement of the dimer due to electrostatic attraction. We can give an estimation of this enlargement. First, we write the energy of an ion of A^- taking into account only their nearest neighbours as a function of the displacement from the equilibrium position of the covalent A–A bond (δ), and keep only terms of second order in δ. Then, we obtain the value of δ which minimizes that energy. As long as we want to obtain a numerical value for δ, first we must give an estimation of the Hooke constant for the parabolic potential well of the covalent A–A bonding. For example, in the case of NiS_2, we will calculate the Hooke constant as the height of the potential well (the value of the formation energy of the molecule S_2 [21]) over the square of the maximum enlargement to break the covalent bond (we take 10% of the covalent radius), giving ≈3500 J m^{-2}. Then, $\delta_{min} \approx 0.024$ Å, and the enlargement can be estimated as ≈0.05 Å, in good agreement with the observed value of ≈0.06 Å.

According to the usual model [8], the splitting of the e_g band is produced by the interionic interaction energy of the electrons. When an S atom is substituted by one of the Se an increase of the inter-atomic distances is observed (see figure 4). This increase will decrease the overlap integral for electron orbitals and so will cause a decrease of that interionic interaction energy. That may be the reason for samples with $x_{Se} \geqslant 0.6$ being metallic.

5. Conclusions

We have synthesized polycrystalline $NiS_{2-x}Se_x$ thin films by thermal sulphuration and seleniation of Ni thin films in closed ampoules. Different samples have been obtained with x_{Se} values which run through the whole range from 0 to 2.0. Selenium content has been measured by x-ray fluorescence and determined by x-ray diffraction respectively. An study of the sulphuration and seleniation process has been done by comparing the Se molar fraction in gas in the ampoule during the annealing to the selenium content in the sample after the process. Experimental results agree well with a theoretical model developed taking into account the difference in diffusion properties of sulphur and selenium respectively into the nickel film. A relation between sulphur and selenium diffusion of 0.24 fits well with experimental data.

Structural properties have been studied by Rietveld refinement from x-ray diffraction of the samples. A linear relation has been found between lattice parameter and selenium content that corresponds to a Vegard law. Also linear relations with selenium content have been found for anion positional parameter, u, and bond distances in the lattice. Relations between Ni–anion and anion–anion bond distances with selenium content are very similar to those which can be expected from theoretical geometric relations.

Resistivity measurements against temperature reveal the different behaviour between two samples with different selenium concentration. That with a selenium content $x_{Se} = 0.22$ has a semiconducting behaviour all through the temperature range. In contrast, the sample with a selenium content $x_{Se} = 0.40$ has a transition from semiconductor to metallic phase at about 100 K, the same temperature at which a Mott transition has been observed in single

crystal samples [1, 8]. Resistivity measurements in samples with other selenium contents are now in progress.

Acknowledgments

The authors wish to thank Professor S Vieira for his suggestions and for affording us the possibility of making the resistivity measurements at low temperatures in his laboratory, and also to thank Professor F Jaque for a critical reading of the manuscript. The technical assistance of F Moreno is gratefully recognized. This work has been done with the support of the Comision Interministerial de Ciencia y Tecnología (Mat97-1480-E).

References

[1] Bouchard R J, Gillson J L and Jarret H S 1973 *Mater. Res. Bull.* **8** 489
[2] Gautier F *et al* 1975 *Phys. Lett.* **53A** 31
[3] Miyadai T, Saitoh M and Tazuke Y 1992 *J. Magn. Magn. Mater.* **104** 1953
[4] Thio T and Bennett J W 1994 *Phys. Rev.* B **50** 10 574
[5] Wilson J A and Pitt G D 1971 *Phil. Mag.* **23** 1297
[6] Jarnett H S, Bouchard R J, Gillson J L, Jones G A, Marcus S M and Weiher J F 1973 *Mater. Res. Bull.* **8** 877
[7] Krill G, Lapierre M F, Gautier F, Robert C, Czjzek G, Fink J and Schmidt H 1976 *J. Phys. C: Solid State Phys.* **9** 761
[8] Kwizera P, Dresselhaus M S and Adler D 1980 *Phys. Rev.* B **21** 2328
[9] Takano H and Okiji A 1981 *J. Phys. Soc. Japan* **50** 3835
[10] Sudo S and Miyadai T 1985 *J. Phys. Soc. Japan* **54** 3934
[11] Matsuura A Y, Shen Z X, Dessau D S, Park C H, Thio T, Bennet J W and Jepsen O 1996 *Phys. Rev.* B **53** R7584
[12] de las Heras C, Martín de Vidales J L, Ferrer Y J and Sánchez C 1996 *J. Mater. Res.* **11** 211
[13] Drowart J, Goldfinger P, Detry D, Rickert H and Keller H 1967 *Adv. Mass Spectrosc.* **4** 499
[14] Berkowitz J and Chupka W A 1966 *J. Chem. Phys.* **45** 4289
[15] Sakthiveld A and Young R A 1991 *User Guide to Programs DBWS-9006 and DBWS-9006PC for Rietveld Analysis of X-ray and Neutron Powder Diffraction Patterns* (Atlanta, GA: School of Physics, Georgia Institute of Technology)
[16] Caglioti G, Paoletti A and Ricci F P 1958 *Nucl. Instrum.* **3** 223
[17] Gmelin E, Alpen U v *5th Int. Cryogenic Engineering Conf.*
[18] Mayadas A F and Shatzkes M 1970 *Phys. Rev.* B **1** 1382
[19] Volger J 1950 *Phys. Rev.* **79** 1023
Petriz R L 1956 *Phys. Rev.* **104** 1508
[20] Prutton M 1975 *Surface Physics* (Oxford: Clarendon)
[21] 1986–87 *CRC Handbook Chemistry and Physics* 67th edn (Boca Raton, FL: Chemical Rubber Company)